

sheets) and by estimating the average egg density per clutch (measured from 50 clutches using macro-photography).

Fully developed larvae of *P. amboinensis* settle onto reefs at night after a restricted period of 18–21 days in the plankton^{25,26}. At this time they are easily identified and strongly attracted to light, so they can readily be collected at night using light traps²⁷. Four light traps were placed at a windward site, two in the lagoon and two at a back-reef location between 21 October and 21 January, in order to sample juveniles returning to different reef zones (Fig. 1).

The calculation of the proportion of the total number of embryos produced at Lizard Island that were marked is based on the size of the six areas in which all the embryos were marked, as a proportion of an estimate of the total suitable breeding habitat at Lizard Island. The area of suitable breeding habitat was assumed to be proportional to the length of the reef-edge habitat (a total of 900 m for marking sites). The length of all reef-edge habitat was measured from an aerial photograph (scale 1 : 7500) using a digitizing tablet. The upper limit excluded all adjacent reef habitats within 500 m that were separated from Lizard Island by stretches of sand, and the lower limit included such reefs.

The calculation of M_e/T_e (Box 1) using relative breeding area assumes that: (1) All embryos produced at the six marking sites over the three months were actually marked. This can be substantiated as all females laid their eggs on tiles and all tiles with eggs were immersed every two days. Also, the pilot study showed that immersion in tetracycline for 1 h is 100% successful. (2) The relative sizes of the areas in which marking was and was not carried out reflect the difference in egg production between the two areas. There were no significant differences in mean clutch size or female density where tiles were present and where they were absent. Mean clutch size = 4.969 (± 535 s.e.) at the six marking sites and 5.237 (± 625 s.e.) at three non-marking sites; mean female density = 17.5 (± 3.5 s.e.) per 100 m² at the six marking-sites and 18.4 (± 3.1 s.e.) at three non-marking sites. (3) There was no difference in the mortality rates and/or recapture probabilities of marked and unmarked embryos. Our pilot study showed that at least until hatching, survival rates of marked and unmarked embryos were not statistically different. In the three-month study only 12 PVC tiles over-turned between visits. This only affected five marked clutches. A further five marked clutches appeared to have been decimated by benthic predators. These were not included in the final calculations.

Received 25 March; accepted 25 October 1999.

- Sinclair, M. *Marine Populations: an Essay on Population Regulation and Speciation* (Washington Sea Grant, Seattle, 1988).
- Roughgarden, J., Gaines, S. D. & Pacala, S. W. in *Organization of Communities* (eds Gee, J. H. R. & Giller, P. S.) 491–518 (Blackwell, London, 1987).
- Underwood, A. J. & Fairweather, P. G. Supply-side ecology and benthic marine assemblages. *Trends Ecol. Evol.* **4**, 16–20 (1989).
- Roberts, C. M. Connectivity and management of Caribbean coral reefs. *Science* **278**, 1454–1457 (1997).
- Roberts, C. M. Ecological advice for the global fisheries crisis. *Trends Ecol. Evol.* **12**, 35–38 (1997).
- Fairweather, P. G. Implications of 'supply-side ecology' for environmental assessment and management. *Trends Ecol. Evol.* **6**, 60–63.
- Roberts, C. M. & Hawkins, J. P. Extinction risk in the sea. *Trends Ecol. Evol.* **14**, 241–246.
- Caley, M. J., Carr, M. H., Hixon, M. A., Hughes, T. P., Jones, G. P. & Menge, B. A. Recruitment and the local dynamics of open marine populations. *Annu. Rev. Ecol. Syst.* **27**, 477–500 (1996).
- Thorson, G. Reproductive and larval ecology of marine bottom invertebrates. *Biol. Rev. Cambridge Phil. Soc.* **25**, 1–45 (1950).
- Palumbi, S. R. Genetic divergence, reproductive isolation, and marine speciation. *Annu. Rev. Ecol. Syst.* **25**, 547–572 (1994).
- Shulman, M. J. What can population genetics tell us about dispersal and biogeographic history of coral-reef fishes? *Aust. J. Ecol.* **23**, 216–225 (1998).
- Bell, L. J., Moyer, J. T. & Numachi, K. Morphological and genetic variation in Japanese populations of the anemonefish *Amphiprion clarkii*. *Mar. Biol.* **72**, 99–108 (1982).
- Planes, S. Genetic differentiation in relation to restricted larval dispersal of the convict surgeonfish *Acanthurus triostegus* in French Polynesia. *Mar. Ecol. (Prog. Ser.)* **98**, 237–246 (1993).
- Hourigan, T. F. & Reese, E. S. Mid-ocean isolation and the evolution of Hawaiian reef fishes. *Trends Ecol. Evol.* **2**, 187–191 (1987).
- Baltz, D. M. Introduced fishes in marine systems and inland seas. *Biol. Conserv.* **56**, 151–177 (1991).
- Schultz, E. T. & Cowen, R. K. Recruitment of coral-reef fishes to Bermuda: local retention or long-distance transport? *Mar. Ecol. (Prog. Ser.)* **109**, 15–28 (1994).
- Doherty, P. J. & Carleton, J. M. The distribution and abundance of pelagic juvenile fish near Grub Reef, central Great Barrier Reef. *Proc. 8th Int. Coral Reef Symposium* **2**, 1155–1160 (1997).
- Stobutzki, I. C. & Bellwood, D. R. Nocturnal orientation to reefs by late pelagic stage coral reef fishes. *Coral Reefs* **17**, 103–110 (1998).
- Leis, J. M., Sweatman, H. P. A. & Reader, S. E. What the pelagic stages of coral reef fishes are doing out in blue water: daytime field observations of larval behavioural capabilities. *Mar. Freshwater Res.* **47**, 401–411 (1996).
- Campana, S. E., Neilson, J. D. Microstructure of fish otoliths. *Can. J. Fish. Aquat. Sci.* **42**, 1014–1032.
- Secor, D. H., White, M. G. & Dean, J. M. Immersion marking of larval and juvenile hatchery-produced striped bass with oxytetracycline. *Trans. Am. Fish. Soc.* **120**, 261–266 (1991).
- Secor, D. H. & Houde, E. D. in *Recent Developments in Fish Otolith Research* (eds Secor, D. D., Dean, J. M. & Campana, S. E.) 423–444 (University of South Carolina Press, Columbia, 1995).
- Tsukamoto, K. Otolith tagging of ayu embryo with fluorescent substances. *Nippon Suisan Gakkaishi* **54**, 1289–1295 (1988).
- Reinert, T. R., Wallin, J., Griffin, M. C., Conroy, M. J. & Van Den Avyle, M. J. Long-term retention and detection of oxytetracycline marks applied to hatchery-reared larval striped bass, *Morone saxatilis*. *Can. J. Fish. Aquat. Sci.* **55**, 539–543 (1998).
- Meehan, M. G., Milicich, M. J. & Doherty, P. J. Larval production drives temporal patterns of larval supply and recruitment of a coral reef damselfish. *Mar. Ecol. (Prog. Ser.)* **93**, 217–225 (1993).
- Kerrigan, B. A. Temporal patterns in size and condition at settlement in two tropical reef fishes (Pomacentridae: *Pomacentrus amboinensis* and *P. nagasakiensis*). *Mar. Ecol. (Prog. Ser.)* **135**, 27–41 (1996).

27. Doherty, P. J. Light-traps: selective but useful devices for quantifying the distributions and abundances of larval fishes. *Bull. Mar. Sci.* **41**, 423–431 (1987).

Acknowledgements

We thank I. Key and B. Kerrigan for assistance in the field and laboratory, and M. McCormick and P. Munday for editorial comments. This work was supported by the Australian Research Council, Large Grant Scheme, James Cook University and the Australian Museum's Lizard Island Research Station.

Correspondence and requests for materials should be addressed to G.P.J. (e-mail: geoffrey.jones@jcu.edu.au).

Regulation of lifespan by sensory perception in *Caenorhabditis elegans*

Javier Apfeld & Cynthia Kenyon

Department of Biochemistry and Biophysics, University of California at San Francisco, California 94143-0448, USA

Caenorhabditis elegans senses environmental signals through ciliated sensory neurons located primarily in sensory organs in the head and tail. Cilia function as sensory receptors, and mutants with defective sensory cilia have impaired sensory perception^{1,2}. Cilia are membrane-bound microtubule-based structures and in *C. elegans* are only found at the dendritic endings of sensory neurons³. Here we show that mutations that cause defects in sensory cilia or their support cells, or in sensory signal transduction, extend lifespan. Our findings imply that sensory perception regulates the lifespan of this animal, and suggest that in nature, its lifespan may be regulated by environmental cues.

We determined the lifespans of eleven mutants (in nine genes) with various defects in sensory cilia, including the absence of cilia (*daf-19*), deletion of the middle and distal segments (*che-2*, *che-13*, *osm-1*, *osm-5* and *osm-6*) and reduced or irregular ciliary segments (*che-3*, *che-11* and *daf-10*). One of these genes, *osm-6*, has been cloned. *osm-6* is expressed only in ciliated neurons⁴, and encodes a homologue of the *Chlamydomonas reinhardtii* intraflagellar transport particle, required for assembly of the flagellum, a cilium-like structure⁵. We found that all of these mutants were long lived (Fig. 1; Table 1). Thus, the function of sensory cilia is required for *C. elegans* to age normally.

Sensory cilia are present in 60 of the 302 neurons present in the *C. elegans* hermaphrodite³. The amphids, a pair of lateral sensilla in the head, are the principal sensory organs. Each amphid contains the ciliated endings of twelve sensory neurons, plus a sheath and a socket cell, which form a pore to the exterior. The phasmids are similar but smaller sensory organs in the tail. Four other classes of cuticular sensilla are also located in the head. We determined the lifespans of five mutants in four genes thought to affect only a subset of sensilla. *daf-6(e1377)* mutants, in which the amphid and phasmid pores are closed because of a defect in the sheath cells⁶, were long lived (Fig. 1; Table 1). *mec-8(e398)* mutants, in which amphid sensory cilia partially fail to fasciculate¹, as well as two *osm-3* mutants, in which only the cilia of the phasmid neurons and 16 out of the 24 amphid neurons are defective¹, were also long lived (Fig. 1; Table 1). *osm-3* encodes a kinesin-like protein that is expressed in the 20 ciliated sensory neurons that are affected in the mutant, and in 6 other ciliated sensory neurons that are unaffected in the mutant⁷. The remaining mutant, a *mec-1* mutant that has a relatively weak defect in amphid cilia fasciculation¹, was not long lived (Fig. 1; Table 1). Finally, to test the involvement of the amphids directly, we ablated the two amphid sheath cells with a laser microbeam and found that this treatment also extended lifespan

(Fig. 1; Table 1). Together, these findings suggest that at least some of the neurons whose activity influences lifespan are amphid sensory neurons.

In vertebrate olfactory and visual systems, cyclic nucleotide-gated channels are required to transduce receptor activity into electrical activity⁸. In *C. elegans*, the cyclic nucleotide-gated channel α -subunit TAX-4 and β -subunit TAX-2 function at the ciliated endings of a subset of amphid neurons to mediate several sensory behaviours^{9,10}. *tax-2* and *tax-4* are thought to function directly in sensory transduction⁹; mutations in these genes do not affect the structure of the sensory cilia¹⁰. We tested two *tax-4* alleles and found that both extended lifespan (Fig. 1; Table 1). We also tested three

tax-2 alleles, and found that they had little or no effect on lifespan (Fig. 1; Table 1). TAX-4 is able to form functional channels in the absence of TAX-2 (ref. 11). These findings suggest that a TAX-4-dependent channel that does not require TAX-2 may operate within sensory cilia to regulate lifespan.

We then considered whether cilium structure mutants had any other obvious defects that might influence lifespan. We analysed mutants in five genes, *che-2*, *daf-6*, *daf-10*, *osm-3* and *osm-5*. The feeding behaviours of these mutants were normal. The percentage of animals pumping (a pharyngeal behaviour that draws bacteria into the mouth and intestine¹²) was similar to wild type, as was the rate of pumping in individual animals (Table 2). The mutants were less likely to stray from the bacterial lawns (their food) than were wild-type animals (Table 2); this preference for food may be caused by

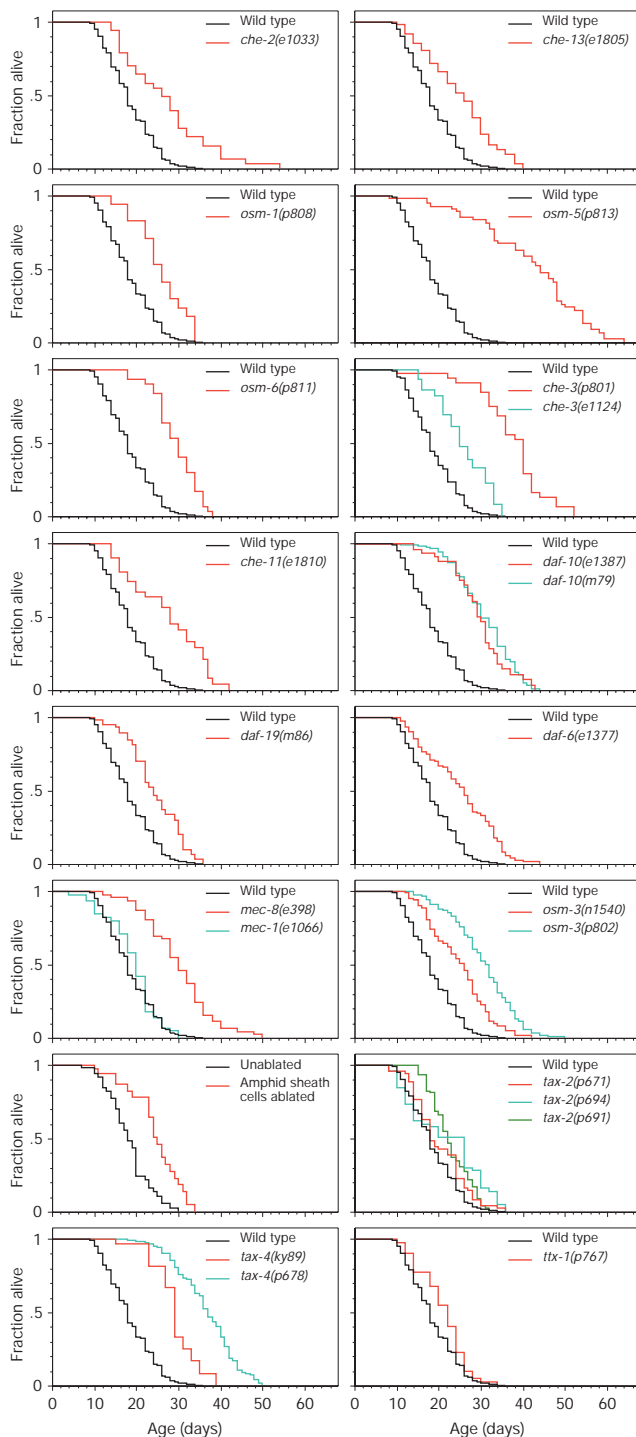


Figure 1 Animals with defects in sensory cilia and sensory transduction live longer than wild type. The fraction of animals remaining alive is plotted against animal age.

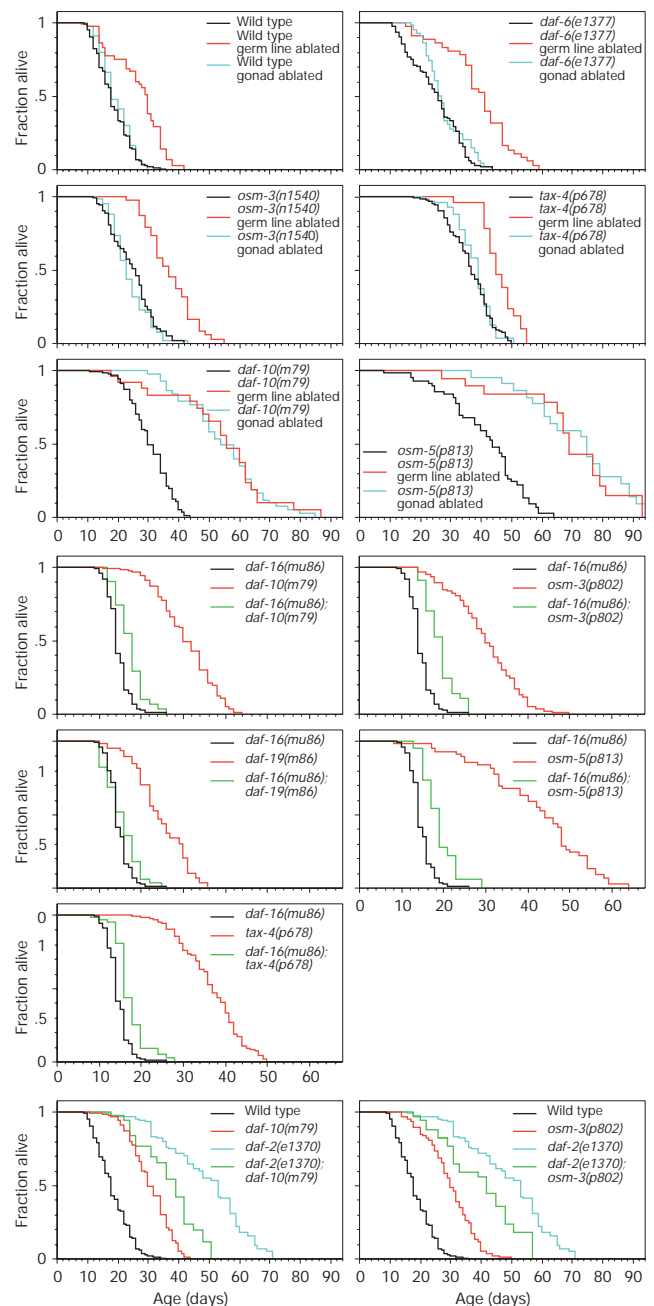


Figure 2 Survival curves of germline- and gonad-ablated animals, and double mutants. The fraction of animals remaining alive is plotted against animal age. The deaths of the last two surviving *osm-5(p813)* gonad-ablated animals are not shown. These animals died when they were 95 and 121 days old.

their altered sensory ability². The mutants had a normal appearance and length of postembryonic development, and they had either normal or slightly elevated brood sizes (Table 2). Because these mutants appeared normal in all of these respects, it is possible that their longevity is caused directly by altered sensory perception.

In *C. elegans*, signals from the reproductive system influence lifespan¹³; the germ line produces signals that shorten lifespan, and the somatic gonad appears to produce counterbalancing signals that lengthen lifespan¹³. We ablated the germline precursors, Z2 and Z3, in five mutants, *daf-6*, *daf-10*, *osm-3*, *osm-5* and *tax-4*, and found that their lifespans were extended (Fig. 2; Table 3). Thus, germline signalling appeared normal. We then removed the entire gonad by killing the somatic gonad precursors, Z1 and Z4. This treatment prevents the development of the germ line, as well as the somatic gonad, and has no effect on wild-type lifespan^{13,14}. Three of the mutants, *daf-6*, *osm-3* and *tax-4*, behaved like wild type; that is, killing the entire gonad had no effect on their lifespans (Fig. 2; Table 3). In contrast, in *daf-10* and *osm-5* mutants, killing the entire gonad lengthened lifespan to the same extent as did killing only the

germ line (Fig. 2; Table 3). Thus, in these mutants, somatic gonad signalling appeared to be silenced. *daf-10* and *osm-5* mutations affect most of the ciliated sensory neurons, whereas *daf-6*, *osm-3* and *tax-4* mutations affect only subsets of these neurons¹⁹. Therefore, it is possible that somatic gonad signalling requires the activity of sensory neurons that are affected in *daf-10* and *osm-5* but not in *daf-6*, *osm-3* or *tax-4* mutants. Alternatively, impaired function of a large number of neurons could be required to silence somatic gonad signalling.

The lifespan of *C. elegans* is thought to be regulated hormonally. Mutations in *daf-2*, which encodes an insulin/IGF-1 receptor homologue, and in downstream signalling components, cause animals to live more than twice as long as wild type^{14,15} (reviewed in ref. 16). This longevity requires DAF-16, a forkhead-family transcription factor^{14,17–20}. *daf-16* also acts in pathways that appear to regulate lifespan independently of *daf-2*, such as the germline signalling pathway¹³.

To investigate the role of *daf-16*, we constructed double mutants between a *daf-16* null allele, *mu86* (ref. 20), and mutations in five genes, *osm-3*, *osm-5*, *daf-10*, *daf-19* and *tax-4*. Loss of *daf-16*

Table 1 Adult lifespans at 20 °C

Strain/treatment	Mean ± s.e.m. (days)	75th percentile (days)*	Number of animals that died/Total†	P
Wild type	18.8 ± 0.3	22	347/531 (11)	
<i>che-2(e1033)</i>	26.8 ± 1.7	32	33/48 (1)	<0.0001‡
<i>che-3(p801)</i>	37.5 ± 1.4	42	31/47 (1)	<0.0001‡
<i>che-3(e1124)</i>	25.7 ± 1.0	31	38/60 (1)	<0.0001‡
<i>che-11(e1810)</i>	27.3 ± 1.6	36	27/49 (1)	<0.0001‡
<i>che-13(e1805)</i>	25.0 ± 1.3	30	36/95 (2)	0.0005, 0.0007§
<i>daf-6(e1377)</i>	25.1 ± 1.0	33	75/101 (2)	<0.0001‡
<i>daf-10(e1387)</i>	29.4 ± 1.2	34	30/100 (2)	<0.0001‡
<i>daf-10(m79)</i>	30.7 ± 0.5	36	137/198 (4)	<0.0001‡
<i>daf-19(mu86)</i>	24.5 ± 1.0	30	35/126 (2)	0.0003, 0.0005§
<i>mec-1(e1066)</i>	19.0 ± 0.4	24	45/49 (1)	0.45
<i>mec-8(e398)</i>	30.0 ± 1.2	34	46/50 (1)	<0.0001‡
<i>osm-1(p808)</i>	25.8 ± 1.4	30	17/54 (1)	<0.0001‡
<i>osm-3(n1540)</i>	24.8 ± 0.8	30	67/101 (2)	<0.0001‡
<i>osm-3(p802)</i>	30.6 ± 0.6	36	133/248 (5)	<0.0001‡
<i>osm-5(p813)</i>	41.6 ± 1.7	50	46/146 (3)	<0.0001‡
<i>osm-6(p811)</i>	29.4 ± 1.0	34	30/48 (1)	<0.0001‡
<i>txx-1(p767)**</i>	21.0 ± 0.9	24	40/49 (1)	0.15
Unablated	18.3 ± 0.8	20	41/60 (1)	
Amphid sheath cells ablated	24.5 ± 1.2	29	23/49 (1)	<0.0001¶
<i>tax-4(p678)</i>	36.6 ± 0.7	42	105/145 (3)	<0.0001‡
<i>tax-4(ky89)</i>	29.1 ± 1.4	33	13/49 (1)	<0.0001‡
<i>tax-2(p671)</i>	20.1 ± 0.9	24	50/61 (1)	0.19
<i>tax-2(p691)</i>	22.7 ± 0.5	27	100/120 (1)	0.34
<i>tax-2(p694)</i>	21.6 ± 1.4	30	44/54 (1)	0.01
<i>daf-16(mu86)</i>	14.5 ± 0.2	16	169/263 (4)	
<i>daf-16(mu86); daf-10(m79)</i>	17.4 ± 0.6	20	31/48 (1)	<0.0001#
<i>daf-16(mu86); daf-19(mu86)</i>	15.3 ± 0.6	18	36/60 (1)	<0.0001, 0.32*
<i>daf-16(mu86); osm-3(p802)</i>	19.2 ± 0.6	20	29/47 (1)	<0.0001‡
<i>daf-16(mu86); osm-5(p813)</i>	18.7 ± 0.6	21	36/60 (1)	<0.0001‡
<i>daf-16(mu86); tax-4(p678)</i>	17.3 ± 0.5	20	45/84 (1)	<0.0001‡
<i>daf-2(e1370)</i>	49.2 ± 1.5	59	82/103 (1)	
<i>daf-2(e1370); daf-10(m79)</i>	37.2 ± 1.8	42	27/49 (1)	<0.0001**
<i>daf-2(e1370); osm-3(p802)</i>	40.0 ± 2.1	48	34/48 (1)	<0.0001**

* The 75th percentile is the age when the fraction of animals alive reaches 0.25.

† The total number of observations equals the number of animals that died plus the number censored. The number of independent times the lifespan was determined is in parenthesis. Animals that crawled off the plate, exploded or bagged were censored at the time of the event. This step incorporated those worms into the data set until the censor date²⁷, and was necessary to avoid the loss of information; for example, if a 50-day-old animal crawls off the plate, it is important to include that information in the data set, as that animal was long lived. Control and experimental animals were cultured in parallel. Many experiments were performed more than once. The logrank (Mantel-Cox) test was used to test the hypothesis that the survival functions among groups were equal. P values were calculated for individual experiments, each consisting of control and experimental animals examined at the same time. We show the cumulative statistics in figures and tables because strains behaved similarly in different experiments. Below, the letters A–K refer to the 11 different experiments we performed; in each experiment, multiple strains were examined in parallel. The P values comparing mean lifespans of the same strain in different experiments were P = 0.40 for wild type (mean lifespans of animals tested in each of 11 individual experiments: A, 17.2 ± 0.9; B, 18.9 ± 0.8; C, 19.7 ± 0.8; D, 18.4 ± 0.9; E, 17.9 ± 0.9; F, 19.0 ± 1.0; G, 17.8 ± 0.8; H, 19.3 ± 1.0; I, 20.5 ± 1.1; J, 18.4 ± 1.1; K, 20.0 ± 1.0); P = 0.20 for *che-13* (means: B, 23.7 ± 1.6; J, 26.2 ± 2.2); P = 0.81 for *daf-6* (means: C, 24.3 ± 1.4; J, 25.8 ± 1.4); P = 0.27 for *daf-10(e1387)* (means: E, 27.5 ± 2.1; J, 30.8 ± 1.3); P = 0.33 for *daf-10(m79)* (means: A, 31.1 ± 1.0; C, 30.0 ± 1.1; G, 29.3 ± 1.3; I, 32.4 ± 0.9); P = 0.92 for *daf-19* (means: E, 24.3 ± 1.4; F, 24.5 ± 1.4); P = 0.02 for *osm-3(n1540)* (means: D, 26.8 ± 1.2; J, 22.7 ± 1.0); P = 0.04 for *osm-3(p802)* (means: A, 29.0 ± 1.4; C, 32.8 ± 1.7; G, 29.1 ± 1.6; I, 29.0 ± 1.2; J, 32.8 ± 1.1); P = 0.60 for *osm-5* (means: B, 40.9 ± 2.8; F, 41.7 ± 2.4; J, 44.9 ± 5.0); P = 0.52 for *tax-4(p678)* (means: I, 36.3 ± 1.6; J, 36.3 ± 1.1; K, 37.1 ± 1.0); and P = 0.38 for *daf-16* (means: C, 14.1 ± 0.2; E, 14.9 ± 0.4; F, 14.7 ± 0.5; J, 14.1 ± 0.4). Strains whose lifespans were determined only once were examined in the following experiments: A, *osm-1*; B, *che-2*; C, *daf-16*; *daf-10*, *daf-16*; *osm-3*; D, *che-3(p801)*, *mec-1*, *mec-8*; E, *che-11*, *osm-6*; F, *daf-16*; *osm-5*, *daf-16*; G, *daf-2*, *daf-2*; *daf-10*, *daf-2*; *osm-3*; J, *txx-1*, *tax-4(ky89)*, *tax-2(p671)*, *tax-2(p691)*, *tax-2(p694)*, *daf-16*; *tax-4*. The experiments in which the germline and gonad ablations were performed (Table 3) were I, *daf-10* and wild type; J, *daf-6*, *osm-3*, *osm-5*, *tax-4* and wild type (for wild type, only intact and germ-line-ablated animals were examined in this experiment). The total number of animals was at least 46 for each strain in each experiment.

‡ Compared with wild-type control in all experiments.
§ Compared with wild-type control in two experiments.

|| Compared with wild-type control.

¶ Compared with unablated control.

Compared with cilium-structure mutant control and *daf-16(mu86)* control.

* Compared with *daf-19(mu86)* and *daf-16(mu86)* controls, respectively.

** Compared with cilium-structure mutant control and *daf-2(e1370)* control.

†† In addition, *txx-1(p767)* animals had lifespans that were not significantly different from those of wild type at 15 °C (P = 0.03) and 25 °C (P = 0.37).

Table 2 Phenotypic characterization of cilium-structure mutants

Genotype	Percentage of animals on the bacterial lawn*	Feeding rate (pumps per minute)†	Percentage of animals pumping*	Length of postembryonic development (h)‡	Brood size‡
Wild type	65% (312)	206 ± 12 (20)	100% (320)	44.8 ± 1.1 (18)	280 ± 18 (11)
<i>che-2(e1033)</i>	81% (110)	210 ± 12 (5)	100% (110)	44.1 ± 2.4 (37)	272 ± 36 (9)
<i>daf-6(e1377)</i>	90% (104)	210 ± 14 (5)	100% (100)	44.9 ± 1.3 (31)	327 ± 20 (12)
<i>daf-10(m79)</i>	85% (113)	204 ± 15 (5)	100% (340)	45.1 ± 1.7 (40)	306 ± 10 (12)
<i>osm-3(p802)</i>	80% (71)	208 ± 8 (5)	100% (180)	44.6 ± 1.0 (36)	294 ± 31 (12)
<i>osm-5(p813)</i>	83% (174)	210 ± 14 (5)	100% (245)	44.9 ± 1.5 (17)	321 ± 31 (12)

Fisher's exact tests were conducted to determine the probability that the observed differences in the percentage of animals on the bacterial lawn were due to chance. Unpaired *t*-tests were conducted to determine the probability that the observed differences in mean feeding rate, mean length of postembryonic development and mean brood size between two groups were due to chance. With two exceptions, no statistical significance was observed when comparing wild type with any group ($P > 0.1$). The measured mean brood sizes of *daf-6* ($P < 0.0001$), *daf-10* ($P = 0.0002$) and *osm-5* ($P = 0.0008$) were larger than wild type, and the fractions of *che-2* ($P = 0.0002$), *daf-6* ($P < 0.0001$), *daf-10* ($P < 0.0001$), *osm-3* ($P = 0.012$) and *osm-5* ($P < 0.0001$) mutants located on the bacterial lawn were greater than wild type.

* Number of one-day-old adult animals assayed is in parentheses.

† Mean ± s.d. Number of trials is in parentheses. Each trial represents the number of pumps observed in a one-day-old adult animal in 1 min.

‡ Mean ± s.d. Number of animals assayed is in parentheses.

markedly reduced but, in most cases, did not completely eliminate lifespan extension (Fig. 2; Table 1). Thus, most of this lifespan extension requires *daf-16* activity, but a fraction is *daf-16* independent. *daf-16* could act downstream of a sensory signal to regulate lifespan, or it could act in a parallel pathway to provide an activity that these animals simply require for their longevity.

We also determined the lifespans of *daf-2* double mutants. This method has been used to show that the PI3 kinase *age-1* is likely to function in a pathway with *daf-2*, as the double mutant has a lifespan that is similar to those of the single mutants¹⁸. In contrast, the longevity produced by germline ablation appears to be *daf-2* independent, because ablating the germ line in *daf-2* mutants causes an additional doubling of lifespan¹³. We constructed *daf-2(e1370)* double mutants with *daf-10* and *osm-3* mutations. The double mutants did not live longer than the *daf-2(e1370)* single mutant; instead, unexpectedly, their lifespans were slightly shorter than those of *daf-2(e1370)* (Fig. 2, Table 1). A trivial explanation, that the cilium-structure mutations somehow limit the potential lifespan of the animal, seems unlikely, as germline-ablated *daf-10* mutants lived much longer than *daf-2*; *daf-10* double mutants (Fig. 2, Table 3). Thus, we infer that the cilium-structure mutants do not act exclusively in a *daf-2*-independent pathway. To reconcile these findings, we propose the model that sensory neurons do act in a *daf-2*-dependent pathway, but that they also affect the animal in another way. Specifically, we suggest that an environmental signal perceived by sensory cilia regulates a DAF-2 ligand. In cilium-structure mutants, the level of this ligand falls and lifespan is

extended. In addition, we propose that the cilium-structure mutants produce a second, weaker signal that shortens lifespan. In this model, if a *daf-2* mutation completely mimics the lifespan-extending effect of the cilium-structure mutants, but does not completely block the effect of the lifespan-shortening signal, the double mutants would have a lifespan that is shorter than that of the *daf-2* single mutant.

Certain long-lived *daf-2* mutants, such as the tyrosine kinase-domain mutant *e1370* (ref. 15), also appear to lack somatic gonad signalling¹³. In contrast, the *daf-2(e1368)* mutant, which has an altered DAF-2 ligand-binding domain¹⁵, has normal somatic gonad signalling¹³. This suggests that DAF-2 can respond to two ligands, one of which is somatic-gonad dependent (and can still bind to the *e1368* receptor), and one of which is not (and cannot activate either mutant receptor)¹³. Perhaps the cilium-structure mutations that block somatic gonad signalling affect both DAF-2 ligands, whereas the cilium-structure mutations that do not block somatic gonad signalling affect only the gonad-independent ligand.

Unlike weak loss of *daf-2* function, which increases adult lifespan, more severe loss of *daf-2* function causes juvenile animals to become dauer larvae²¹, a stress-resistant, developmentally arrested larval form normally induced by food limitation, high temperature and crowding²². The ability of *daf-2* mutants to become dauer larvae requires the activity of *daf-16* (ref. 21). Sensory cilia are also involved in the regulation of dauer larva formation^{1,6}, and cilium-structure and *tax-4* mutations are known to interact genetically with other mutations in genes that affect dauer larva formation^{6,21,23,24}.

Table 3 Adult lifespans of germline-ablated and gonad-ablated animals at 20 °C

Strain/treatment	Mean ± s.e.m. (days)	75th percentile (days)	Number of animals that died/total	<i>P</i> *
Wild type	18.4 ± 0.3	22	347/531 (11)	
Wild type germline ablated	26.9 ± 1.1†	34	49/112 (2)	<0.0001
Wild type gonad ablated	19.5 ± 0.8	24	44/47 (1)	0.30
<i>daf-6(e1377)</i>	25.1 ± 1.0	33	75/101 (2)	
<i>daf-6(e1377)</i> germline ablated	39.0 ± 1.7	47	39/66 (1)	<0.0001
<i>daf-6(e1377)</i> gonad ablated	28.1 ± 0.9	33	57/81 (1)	0.20
<i>osm-3(n1540)‡</i>	24.8 ± 0.8	30	67/101 (2)	
<i>osm-3(n1540)</i> germline ablated	37.2 ± 1.2	43	57/62 (1)	<0.0001
<i>osm-3(n1540)</i> gonad ablated	24.1 ± 0.8	27	38/54 (1)	0.27
<i>tax-4(p678)</i>	36.6 ± 0.7	42	105/145 (3)	
<i>tax-4(p678)</i> germline ablated	46.1 ± 1.2	49	22/51 (1)	<0.0001
<i>tax-4(p678)</i> gonad ablated	38.1 ± 0.7	43	60/67 (1)	0.52
<i>daf-10(m79)</i>	30.7 ± 0.5	36	137/198 (4)	
<i>daf-10(m79)</i> germline ablated	53.9 ± 3.5	62	22/47 (1)	<0.0001
<i>daf-10(m79)</i> gonad ablated	54.6 ± 2.0	64	43/60 (1)	<0.0001
<i>osm-5(p813)</i>	41.9 ± 1.8	50	48/146 (3)	
<i>osm-5(p813)</i> germline ablated	68.6 ± 4.3	86	15/35 (1)	<0.0001
<i>osm-5(p813)</i> gonad ablated	72.8 ± 4.0	79	22/48 (1)	<0.0001

Germ line ablated: the germ line precursors Z2 and Z3 were ablated. Gonad Ablated: the somatic gonad precursors Z1 and Z4 were ablated. Killing Z1 and Z4 also blocks the development of the germline. The experiments in which these ablations were performed are listed in the legend of Table 1.

* *P* values were calculated for individual experiments, each consisting of unablated controls and experimental animals examined at the same time.

† Means were: experiment I, 25.8 ± 1.6 and experiment J, 28.2 ± 1.6, $P = 0.41$.

‡ We also ablated the gonads of *osm-3(p802)*; these animals had lifespans that were similar to those of unablated controls ($P = 0.69$, mean = 29.0 ± 1.2, dead/total = 28/47). We were unable to estimate the lifespan of *osm-3(p802)* germ-line-ablated animals, as most of the animals were censored due to explosions.

Table 4 Percentage of animals that formed dauers at 27 °C

Genotype	% Dauer 27 °C*
Wild type	5 ± 2 (22, n = 611)
<i>age-1(hx546)</i>	97 ± 2 (22, n = 349)
Sensory cilia mutants	
<i>che-2(e1033)</i>	97 ± 3 (2, n = 29)
<i>che-3(p801)</i>	31 ± 13 (2, n = 58)
<i>che-3(e1124)</i>	89 ± 7 (2, n = 49)
<i>che-11(e1810)</i>	96 ± 0 (2, n = 52)
<i>che-13(e1805)</i>	98 ± 2 (2, n = 56)
<i>daf-10(m79)</i>	90 ± 2 (4, n = 103)
<i>osm-1(p808)</i>	94 ± 6 (2, n = 55)
<i>osm-3(n1540)</i>	50 ± 3 (3, n = 69)
<i>osm-5(p813)</i>	100 ± 0 (4, n = 104)
<i>osm-6(p811)</i>	100 ± 0 (2, n = 57)
Sheath cells mutant	
<i>daf-6(e1377)</i>	0 ± 0 (2, n = 65)
Cilia fasciculation mutants	
<i>mec-1(e1066)</i>	10 ± 6 (2, n = 44)
<i>mec-8(e398)</i>	2 ± 2 (2, n = 48)
Sensory transduction mutants	
<i>tax-4(p678)</i>	77 ± 7 (4, n = 119)
<i>tax-4(ky89)</i>	100 ± 0 (4, n = 120)
<i>daf-16</i> mutants	
<i>daf-16(mu86)</i>	0 ± 0 (6, n = 170)
<i>daf-16(mu86); daf-10(m79)</i>	0 ± 0 (2, n = 44)
<i>daf-16(mu86); osm-5(p813)</i>	0 ± 0 (2, n = 55)
<i>daf-16(mu86); tax-4(p678)</i>	0 ± 0 (10, n = 300)

* Mean ± s.e.m. Number of trials and total number of animals tested (n) shown in parentheses.

Some mutations have been shown to cause dauer formation at relatively high temperature, 27 °C (refs 16, 25), including cilium-structure mutants (J. Thomas, personal communication). We confirmed this, and found that *tax-4* mutants also formed dauer larvae constitutively at 27 °C. This dauer-formation phenotype, like that of *daf-2*, was *daf-16* dependent in each of three mutants, *osm-5(p813)*, *daf-10(m79)* and *tax-4(p678)* that we tested (Table 4). This suggests that, during dauer formation, sensory input regulates the activity of *daf-16*, possibly by changing the level of *daf-2* activity. This 27 °C dauer phenotype was not observed in mutants with defects in sheath cells or cilia fasciculation (Table 4); thus, the roles of sensory structures in dauer formation and adult lifespan can be uncoupled.

In summary, our findings suggest that perception of an environmental signal may regulate the lifespan of *C. elegans*. What might this signal be? The amphid neurons mediate responses to temperature, volatile and soluble odorants, and mechanical stimuli. It is unlikely that the signal is only temperature, because *ttx-1* mutants, which lack the sensory endings of the amphid finger cells that mediate thermotaxis¹, have normal lifespans (Fig. 1; Table 1). In addition, the amphid finger cells are not affected by *osm-3* mutations¹, which do affect lifespan. The signal affecting lifespan may be a substance that the animal can smell or taste. For example, it may be a pheromone such as dauer pheromone, which reflects population density²², or a compound that originates from organic material and reflects food availability.

Our findings indicate that the ageing process of *C. elegans* is quite plastic and can be affected by signals from sources that would seem to be particularly relevant to its survival and reproductive success: its environment and its reproductive system. Moreover, sensory perception may affect reproductive signalling. Under laboratory conditions, the germ lines and somatic gonads of normal animals appear to produce counterbalancing signals¹³. In this situation, perturbations that retard the development or activity of the germ line but not the somatic gonad might lengthen lifespan, thus, possibly increasing the chances that the animal is still youthful enough to bear progeny when its germ line matures. Perhaps other environmental conditions mimic *daf-10* and *osm-5* mutations, in which germline signals are no longer counterbalanced by somatic gonad signals. Under these conditions, the ageing process could become much more sensitive to general perturbations affecting reproduction. □

Methods

Lifespan analysis

Lifespan assays were conducted at 20 °C as described^{13,26}; at the L4 moult, animals were transferred to plates containing 16 μM 5-fluoro-2'-deoxyuridine (FUDR, Sigma), which kills their progeny as embryos. Control experiments indicated that FUDR does not significantly affect lifespan. We used the L4 moult as *t* = 0 for lifespan analysis. Strains were grown at 20 °C for at least two generations before lifespan determination. A major cause of censoring was explosion, which generally occurred around day 10 of adulthood. In general, the pattern of censoring was not different among strains, except for *daf-19* and *osm-5* mutants, which were more likely to crawl off the plate. In addition, we were unable to estimate the lifespan of the *che-14(e1960)* mutants, because almost all animals exploded. We used Statview 5.0.1 (SAS) software to carry out statistical analysis, and to determine means and percentiles. Censored animals were incorporated into the data set as described²⁷.

Laser ablations

L1 larvae were mounted on 2%-agarose pads containing 1–4 μM NaN₃ as an anaesthetic within an hour of hatching. The amphid sheath cells (AMshL and AMshR) or gonad precursors were killed with a laser microbeam as described¹³. Unablated control animals were treated identically but no cells were killed. In separate controls, the AMshL and AMshR cell deaths were confirmed by the absence of DiI (1,1'-diiododecyl-3,3',3'-tetramethylindocarbocyanine perchlorate, Molecular Probes) dye filling in amphid neurons⁴.

Strain construction

In double-mutant construction, cilium-structure mutants were assayed by the inability of the amphid and phasmid neurons to fill with the dye DiI. *daf-2(e1370)* and *tax-4(p678)* were assayed by the presence of dauers at 25 °C and 27 °C, respectively. *daf-16(mu86)* and *daf-16(+)* were distinguished by PCR using allele-specific primers²⁰. *daf-16(mu86)* is not *Dyf* and did not suppress the *Dyf* defect of *daf-10(m79)*, *daf-19(m86)*, *osm-3(p802)* or *osm-5(p813)* mutants.

Other assays

For dauer assays, animals born at 20 °C were transferred onto a new well-seeded plate as eggs and incubated at 27 °C for 48 h. All other assays were conducted at 20 °C. To measure brood size, two (or in some cases one) L4 animals were cultured together and transferred to new plates every day or every 12 h, and their progeny counted. A set of reserve animals was cultured and transferred in parallel. In the case of *osm-5* (but not the other mutants we examined), animals whose progeny were we counting sometimes crawled off the plates. When this happened, the plate was replaced with another containing age-matched reserve animals, and their subsequent progeny were then counted. We used *F*-tests to compare the variance of the mean brood sizes and found no statistical difference when comparing wild type with any group (*P* > 0.05 in all cases). Pharyngeal pumping was assayed using a dissecting microscope. To determine the length of postembryonic development, larvae that hatched within an hour were monitored every 2 h as they neared adulthood and were scored as adults when they had undergone the final moult and a vulva could be observed.

Received 6 September; accepted 12 October 1999.

- Perkins, L. A., Hedgecock, E. M., Thomson, J. N. & Culotti, J. G. Mutant sensory cilia in the nematode *Caenorhabditis elegans*. *Dev. Biol.* **117**, 456–487 (1986).
- Peckol, E. L., Zallen, J. A., Yarrow, J. C. & Bargmann, C. I. Sensory activity affects sensory axon development in *C. elegans*. *Development* **126**, 1891–1902 (1999).
- White, J. G., Southgate, E., Thomson, J. N. & Brenner, S. The structure of the nervous system of the nematode *C. elegans*. *Phil. Trans R. Soc. Lond. B* **314**, 1–340 (1986).
- Collet, J., Spike, C. A., Lundquist, E. A., Shaw, J. E. & Herman, R. K. Analysis of *osm-6*, a gene that affects sensory cilium structure and sensory neuron function in *Caenorhabditis elegans*. *Genetics* **148**, 187–200 (1998).
- Cole, D. G. *et al.* Chlamydomonas kinesin-II-dependent intraflagellar transport (IFT): IFT particles contain proteins required for ciliary assembly in *Caenorhabditis elegans* sensory neurons. *J. Cell Biol.* **141**, 993–1008 (1998).
- Albert, P., Brown, S. & Riddle, D. Sensory control of dauer larva formation in *Caenorhabditis elegans*. *J. Comp. Neurol.* **198**, 435–451 (1981).
- Tabish, M., Siddiqui, Z. K., Nishikawa, K. & Siddiqui, S. S. Exclusive expression of *C. elegans osm-3* kinesin gene in chemosensory neurons open to the external environment. *J. Mol. Biol.* **247**, 377–389 (1995).
- Zagotta, W. N. & Siegelbaum, S. A. Structure and function of cyclic nucleotide-gated channels. *Annu. Rev. Neurosci.* **19**, 235–263 (1996).
- Komatsu, H., Mori, I., Rhee, J. S., Akaike, N. & Ohshima, Y. Mutations in a cyclic nucleotide-gated channel lead to abnormal thermosensation and chemosensation in *C. elegans*. *Neuron* **17**, 707–718 (1996).
- Coburn, C. M. & Bargmann, C. I. A putative cyclic nucleotide-gated channel is required for sensory development and function in *C. elegans*. *Neuron* **17**, 695–706 (1996).
- Komatsu, H. *et al.* Functional reconstitution of a heteromeric cyclic nucleotide-gated channel of *Caenorhabditis elegans* in cultured cells. *Brain Res.* **821**, 160–168 (1999).
- Avery, L. & Horvitz, H. R. Pharyngeal pumping continues after laser killing of the pharyngeal nervous system of *C. elegans*. *Neuron* **3**, 473–485 (1989).
- Hsin, H. & Kenyon, C. Signals from the reproductive system regulate the lifespan of *C. elegans*. *Nature* **399**, 362–366 (1999).
- Kenyon, C., Chang, J., Gensch, E., Rudner, A. & Tabtiang, R. A *C. elegans* mutant that lives twice as long as wild type. *Nature* **366**, 461–464 (1993).

15. Kimura, K. D., Tissenbaum, H. A., Liu, Y. & Ruvkun, G. *daf-2*, an insulin receptor-like gene that regulates longevity and diapause in *Caenorhabditis elegans*. *Science* **277**, 942–946 (1997).
16. Paradis, S., Ailion, M., Toker, A., Thomas, J. H. & Ruvkun, G. A PDK1 homolog is necessary and sufficient to transduce AGE-1 PI3 kinase signals that regulate diapause in *Caenorhabditis elegans*. *Genes Dev.* **13**, 1438–1452 (1999).
17. Larsen, P. L., Albert, P. S. & Riddle, D. L. Genes that regulate both development and longevity in *Caenorhabditis elegans*. *Genetics* **139**, 1567–1583 (1995).
18. Dorman, J. B., Albinder, B., Shroyer, T. & Kenyon, C. The *age-1* and *daf-2* genes function in a common pathway to control the lifespan of *Caenorhabditis elegans*. *Genetics* **141**, 1399–1406 (1995).
19. Ogg, S. *et al.* The fork head transcription factor DAF-16 transduces insulin-like metabolic and longevity signals in *C. elegans*. *Nature* **389**, 994–999 (1997).
20. Lin, K., Dorman, J. B., Rodan, A. & Kenyon, C. *daf-16*: an HNF-3-forkhead family member that can function to double the life-span of *Caenorhabditis elegans*. *Science* **278**, 1319–1322 (1997).
21. Riddle, D., Swanson, M. & Albert, P. Interacting genes in nematode dauer larva formation. *Nature* **290**, 668–671 (1981).
22. Golden, J. & Riddle, D. The *Caenorhabditis elegans* dauer larva: developmental effects of pheromone, food, and temperature. *Dev. Biol.* **102**, 368–378 (1984).
23. Vowels, J. & Thomas, J. Genetic analysis of chemosensory control of dauer formation in *Caenorhabditis elegans*. *Genetics* **130**, 105–123 (1992).
24. Coburn, C. M., Mori, I., Ohshima, Y. & Bargmann, C. I. A cyclic nucleotide-gated channel inhibits sensory axon outgrowth in larval and adult *Caenorhabditis elegans*: a distinct pathway for maintenance of sensory axon structure. *Development* **125**, 249–258 (1998).
25. Ailion, M., Inoue, T., Weaver, C. I., Holdcraft, R. W. & Thomas, J. H. Neurosecretory control of aging in *Caenorhabditis elegans*. *Proc. Natl Acad. Sci. USA* **96**, 7394–7397 (1999).
26. Apfeld, J. & Kenyon, C. Cell nonautonomy of *C. elegans daf-2* function in the regulation of diapause and life span. *Cell* **95**, 199–210 (1998).
27. Lawless, J. F. *Models and Methods for Lifetime Data* (Wiley, New York, 1982).

Acknowledgements

We thank J. Whangbo, S. Alper, J. Alcedo, H. Hsin, K. Lin, L. Yang, Q. Ch'ng, A. Dillin, D. Garigan and other members of the Kenyon Lab, as well as members of Cori Bargmann's lab, for stimulating discussions. Some nematode strains were provided by the *Caenorhabditis* Genetics Center, which is funded by the NIH. J.A. was supported by an HHMI Predoctoral Fellowship. This work was supported by a grant from the NIA to C.K.

Correspondence and requests for materials should be addressed to C.K. (e-mail: ckenyon@biochem.ucsf.edu).

.....
Atomic scale movement of the voltage-sensing region in a potassium channel measured via spectroscopy

Albert Cha^{*}, Gregory E. Snyder[†], Paul R. Selvin[†] & Francisco Bezanilla^{*}

^{*} Department of Physiology and Department of Anesthesiology, UCLA School of Medicine, Los Angeles, California 90095, USA

[†] Department of Physics and Biophysics Center, University of Illinois at Urbana-Champaign, Urbana, Illinois 61801, USA

.....
Voltage-gated ion channels are transmembrane proteins that are essential for nerve impulses and regulate ion flow across cell membranes in response to changes in membrane potential. They are made up of four homologous domains or subunits, each of which contains six transmembrane segments^{1,2}. Studies of potassium channels have shown that the second (S2) and fourth (S4) segments contain several charged residues, which sense changes in voltage and form part of the voltage sensor^{3–5}. Although these regions clearly undergo conformational changes in response to voltage^{6–10}, little is known about the nature of these changes because voltage-dependent distance changes have not been measured. Here we use lanthanide-based resonance energy transfer^{11,12} to measure distances between *Shaker* potassium channel subunits at specific residues. Voltage-dependent distance changes of up to 3.2 Å were measured at several sites near the S4 segment. These movements directly correlated with electrical measurements of the voltage sensor, establishing the link between physical changes and electrical charge movement. Measured distance changes suggest that the region associated with the S4 segment undergoes

a rotation and possible tilt, rather than a large transmembrane movement, in response to voltage. These results demonstrate the first *in situ* measurement of atomic scale movement in a transmembrane protein.

Lanthanide-based resonance energy transfer (LRET) is a modification of conventional fluorescence resonance energy transfer in which a long-lived lanthanide donor transfers energy in a distance-dependent manner to a conventional organic fluorescent acceptor^{11,12}. This technique has previously been used to measure Angstrom-scale conformational changes in proteins¹³. Here, specific sites in the channel were fluorescently labelled by substituting a cysteine for a particular residue and attaching cysteine-reactive compounds of either a donor, a terbium-chelate maleimide (TbM), or an acceptor, fluorescein maleimide (FM), to the same site in the four identical subunits of the channel (Fig. 1a; see also Methods).

Although this labelling leads to a heterogeneous population of channels with different numbers of donors and acceptors, associated problems are greatly minimized for three reasons. In LRET, only donor-acceptor pairs generate sensitized emission signals (that is, delayed emission of the acceptor after receiving energy from the donor), and channels that contain all donors or all acceptors do not contribute to the signal^{11,12}. Also, with four-fold symmetry of the channel^{14,15}, there are only two possible intersubunit distances: the distance between residues on neighbouring subunits and the distance between residues across the pore, which are related by the Pythagorean theorem (Fig. 1a). Finally, the labelling is done so that there is typically only one acceptor per channel, which can readily accept energy independently from multiple donors.

Intersubunit distances were examined at specific sites near S2, in the S3–S4 linker and S4, and near the channel pore (Fig. 2, Table 1). The intersubunit distances (Fig. 1c and Methods) were calculated using the time constants of acceptor-sensitized emission and donor emission without an acceptor. Donor lifetime in the absence of an acceptor was independent of voltage at all sites, indicating no significant change in the environment of the caged terbium (data not shown). The sensitized emission displayed two time constants at all sites measured, reflecting two donor-acceptor distances that follow a Pythagorean relationship (Fig. 1c). This verifies that the technique is measuring distances between contiguous subunits and across the pore. The distance measured at F425C across the pore (30 Å) corresponds well to the distance obtained between α -carbons for the homologous residue from the crystal structure of the bacterial analogue, KcsA (29 Å) (ref. 14). This confirms that the technique is capable of obtaining realistic estimates of distance, as the KcsA pore has been shown to be similar to the *Shaker* pore in its ability to bind specific inhibitors of *Shaker*¹⁶. However, LRET, like other energy transfer techniques, is better at measuring relative distances or changes in distance than absolute distances. Potential sources of error, such as anisotropy of the fluorophores and uncertainty in the fluorophore's position with respect to the labelled residue due to the linker, have been addressed (see Methods).

Next, voltage-dependent movements near the voltage-sensing regions were measured by determining intersubunit distances as a function of voltage. Residue S346C demonstrated a robust voltage-dependent change in energy transfer as measured by sensitized emission lifetimes 50 ms after changing the voltage (Fig. 3a). This change is probably consistent with a voltage-dependent movement of ~3.2 Å between S346C residues on contiguous subunits as the channel moves into the open state (Fig. 3b). The voltage-dependent movement of S346C also coincides with the gating charge movement for the same channels, as determined by parameters of a sequential three-state model fit²¹ to both values (Fig. 3c). The striking agreement between the measured distance changes and electrical charge movement strongly indicates that the observed movement of S346C residues is closely correlated with the movement of charged residues involved in channel gating.